

Observation of a mixed vortex chains–vortex lattice phase in tilted magnetic fields in $\text{YBa}_2(\text{Cu}_{1-x}\text{Al}_x)_3\text{O}_{7-\delta}$ single crystals

I. V. Grigorieva* and J. W. Steeds

Physics Department, University of Bristol, Tyndall Avenue, Bristol BS8 1TL, United Kingdom

K. Sasaki

Metal Physics Laboratory, Department of Metallurgy, Nagoya University, Nagoya, Japan

(Received 17 September 1993)

A vortex structure consisting of vortex chains embedded into the flux-line lattice (FLL) has been observed in $\text{YBa}_2(\text{Cu}_{1-x}\text{Al}_x)_3\text{O}_{7-\delta}$ single crystals using the Bitter decoration technique. This structure formed in magnetic fields applied at a high angle, between 50° and 80° , with respect to the \hat{c} axis. Although the vortex chains–FLL mixture looked similar to the vortex structure observed earlier in the highly anisotropic $\text{Bi}_2\text{Sr}_2\text{CaCu}_2\text{O}_{8+\delta}$, its evolution with the tilt angle and the applied field demonstrated that it represents an essentially different vortex state which, unlike $\text{Bi}_2\text{Sr}_2\text{CaCu}_2\text{O}_{8+\delta}$, originates from the attractive vortex-vortex interaction. The coexistence of the vortex chains with the FLL is attributed to an incomplete transition from the isotropic vortex lattice to the pure chain state during the sample cooling, owing to pinning.

One of the most fascinating aspects of the properties of high-temperature superconductors is the very rich behavior of the flux-line lattice (FLL). In particular, a phenomenon of vortex attraction was discovered when a magnetic field is applied at an oblique angle with respect to the principal anisotropy axes. Calculations based on the three-dimensional (3D) anisotropic London equations^{1–3} have shown that, as a result of the tendency of vortex currents to stay in the Cu-O planes, one of the magnetic-field components (inside a vortex) becomes negative, bringing about an attractive vortex-vortex interaction within the (\mathbf{B}, \hat{c}) plane. As a result, a highly distorted FLL is formed, with one of the lattice vectors, oriented parallel to the (\mathbf{B}, \hat{c}) plane, significantly shorter than the others. This state of the FLL is referred to as one of “vortex chains.” Recently, a pinstripe pattern of vortex chains was indeed observed by the decoration technique in twin-free single crystals of $\text{YBa}_2\text{Cu}_3\text{O}_{7-\delta}$ (YBCO).⁴ However, similar decoration experiments on the more anisotropic $\text{Bi}_2\text{Sr}_2\text{CaCu}_2\text{O}_{8+\delta}$ (BSCCO) (Ref. 5) revealed a rather different vortex phase, which remains puzzling. Although the vortex chains were formed, they were embedded in the oriented FLL. In addition, their evolution with the tilt angle and the applied field was essentially different from the chain state in YBCO and contradictory to what is expected from the attractive vortex-vortex interaction. Recently, at least two suggestions were put forward in order to explain the “mixed phase” in BSCCO. Both assume a coexistence of two types of vortices: one, parallel to the main anisotropy axis, \hat{c} , and the other, parallel to the (ab) plane,⁶ or one, parallel to \hat{c} and the other, tilted (parallel to the applied field).⁷ Such a split of the applied field into two components may become possible for layered materials with very high anisotropy, like BSCCO or TBCCO.^{7,8} Further experimental evidence is needed to prove that this is the case.

Here we report observations by the Bitter decoration technique of yet another vortex chain state in tilted magnetic fields. It shares some of the characteristics of the

other two vortex states: the vortex chains coexist with the intervening FLL, as in the case of BSCCO, but their evolution with the tilt angle and the applied field is consistent with an attractive vortex-vortex interaction, as in the case of YBCO.

Samples in this study were $\text{YBa}_2(\text{Cu}_{1-x}\text{Al}_x)_3\text{O}_{7-\delta}$ (Al-YBCO) single crystals with $x = 0.04$. It is now well established that doping of YBCO with trivalent elements (Al, Fe, Co) causes transformation of the well-known twin structure into the tweed structure for dopant concentration $x > 0.02$ – 0.03 .⁹ From high-resolution electron microscopy studies it is believed that the tweed structure corresponds to microtwinning, preferentially along $\langle 110 \rangle$, but with the size of orthorhombic domains less than 10 nm. The dopant atoms substitute primarily at the Cu(1) sites in the CuO chains causing some local disorder brought about by the tendency to increase their oxygen coordination from 2 to 3. This structural transformation, in turn, results in a decrease of the critical temperature and the upper critical field H_{c2} (Ref. 10) and the critical currents (Ref. 11) (the effects are similar for all three dopant elements). The crystals in the present study were platelets with the short side parallel to the \hat{c} axis and typical sizes $2 \times 2 \times 0.05$ – 0.1 mm. Details of the crystal growth were published elsewhere.¹² The homogeneity and microstructure of the samples were verified by transmission electron microscopy (TEM) and x-ray diffraction. To further characterize our samples, we performed dc magnetization measurements in a vibrating sample magnetometer. The critical currents were calculated from the irreversible magnetization using the Bean model:¹³ $J_c = 30\Delta M/d$ (here M is the width of the hysteresis loop for the increasing and decreasing fields in emu/cm^3 , d is the sample thickness). Typical values were: $J_c(0, 4.2 \text{ K}) \approx 3.10^3 \text{ A/cm}^2$, $J_c(0, 50 \text{ K}) \approx 10 \text{ A/cm}^2$, which are at least two orders of magnitude lower than J_c for pure YBCO. Such a remarkable decrease of the critical currents in the doped YBCO is believed to be a result of the suppression of the upper criti-

cal field H_{c2} , rather than of a change in the crystal microstructure.¹¹

Details of the high-resolution Bitter technique are described in Ref. 14. All the decorations were performed at 4.2 K, in the field-cooling regime. Figure 1 shows a FLL image obtained with magnetic field applied parallel to the \hat{c} axis. The FLL is isotropic, consistent with the quasitragonality of the tweed structure,¹⁴ and fairly disordered. To implement the tilted field geometry, the samples were mounted with the \hat{c} axis tilted at an angle with respect to the applied magnetic field. About 20 decorations were performed for the tilt angles $\varphi = 20^\circ - 80^\circ$ and the applied fields $H_{\text{ext}} = 10 - 60$ Oe. The average vortex density at the crystal surface, measured on the decoration patterns, was induced by the normal component of the applied field $B_0 = B_{\text{ext}} \cos \varphi$ as always the case in such experiments.^{4,5,15} For tilt angles between 50° and 80° , the isotropic and randomly oriented FLL was replaced by a mixture of vortex chains, running approximately parallel to the (\mathbf{B}, \hat{c}) plane, and the intervening FLL oriented with one of its close-packed vortex rows parallel to the chains. Figure 2 shows typical patterns for the tilt angles 63° and 80° and the same value of B_0 . For $\varphi < 70^\circ$ the chains were typically not straight and somewhat irregular, as in Fig. 2(a), and so were the close-packed vortex rows in the FLL locked between the chains. With increase of the tilt angle (for $\varphi = 75^\circ - 80^\circ$) the chains became more regular, with the same number of the FLL vortex rows between them, over the sample [just one row for 80° , the highest tilt angle for which we have successful decorations—see Fig. 2(b)]. The spacings between the vortices organized in chains were constant over the sample. The deviations which occurred were usually associated with the small defects on the crystal surface. We were able to resolve individual vortices in decoration patterns for $B_0 \leq 17$ G (corresponding to an average vortex spacing $a_0 \geq 1.18 \mu\text{m}$). In larger fields, the images of vortices, especially those in the chains, started to overlap.

The evolution of the chains with tilt angle and applied magnetic field is summarized in Fig. 3. The vortex spacings along the chains, a_c , depend strongly on the tilt angle showing a pronounced minimum for $\varphi = 63^\circ$. At the same time they are practically independent of the external field, except for very low fields, $B_0 < 6$ G, where a_c in-

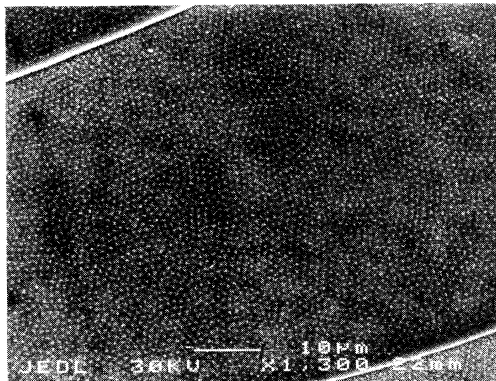


FIG. 1. Scanning electron microscopy (SEM) micrograph of the FLL in the magnetic field of 20 G applied parallel to the \hat{c} axis.

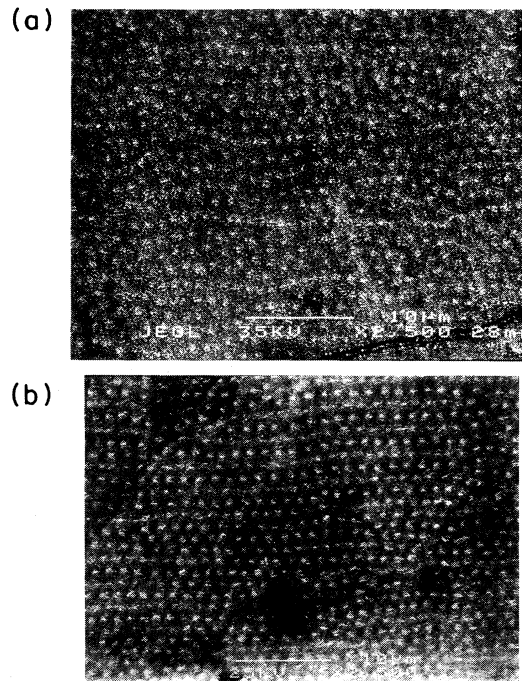


FIG. 2. SEM images of the vortex chains-FLL mixture for the same normal component of the applied field, $B_0 \approx 10$ G, and two tilt angles: (a) $\varphi = 63^\circ$, (b) $\varphi = 80^\circ$. The (\mathbf{B}, \hat{c}) plane in the micrographs is horizontal.

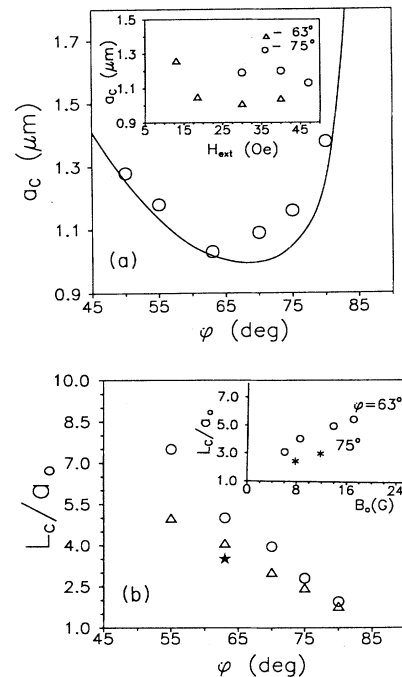


FIG. 3. (a) The intra-chain vortex spacings vs tilt angle for the normal component of the applied field $B_0 \approx 10$ G (open circles). The solid curve is explained in the text. Inset: Intra-chain spacing vs the applied field. (b) The average number of vortex rows locked between the chains vs tilt angle: (\circ) $B_0 \approx 14$ G; (Δ) $B_0 \approx 10$ G; ($*$) $B_0 = 6.8$ G and vs applied field (inset).

creases noticeably. The distance between the chains, L_c , also depends strongly on the tilt angle, decreasing monotonically with increasing φ , and showing an approximately linear dependence on the applied field. The solid curve in Fig. 3(a) is the equilibrium dependence defined by the attractive part of vortex-vortex interaction calculated in Ref. 2 for an anisotropy of $\gamma = (m_c/m_{ab})^{1/2} = 5$ [m_c and m_{ab} are effective masses of the superconducting electrons along the \hat{c} axis and in the (ab) plane, respectively]. The fitting parameter here is the value of λ_{ab} taken as 300 nm. This value, which is much larger than the low-temperature λ_{ab} known from the literature, implies that the vortex patterns we observe at 4.2 K are actually frozen in at a much higher temperature (T^*). Detailed analysis of how this temperature can be estimated is given in Ref. 4 and we will not repeat it here. Unfortunately, we do not know the exact value of $\lambda_{ab}(0)$ for our samples because it is affected by doping. The only relevant data known to us are for the Co-doped YBCO:¹⁶ $\lambda_{ab}(0) = 200$ nm for a concentration of $x = 0.04$. Assuming that Al doping has a similar effect on λ_{ab} (by analogy with other characteristics such as T_c , J_c , etc.) and using the temperature dependence of λ measured in Ref. 16, we obtain $T^*/T_c \approx 0.81 - 0.82$.

Thus, the chain state in our Al-YBCO crystals represents a new vortex phase which can be described as intermediate between the two phases already found. The facts that the whole structure is defined mainly by the tilt angle, and that the $a_c(\varphi)$ dependence shows a pronounced minimum, suggest that the formation of chains in our samples is caused by anisotropy-induced vortex-vortex attraction, i.e., has the same origin as the pinstripe vortex pattern in pure YBCO.⁴ At the same time, the coexistence of the chains with an intervening FLL makes it look similar to the vortex state in BSCCO.⁵ However, there are two important differences from the latter case: first, for Al-YBCO, the intrachain vortex spacings change nonmonotonically with the tilt angle and are only weakly dependent on the applied field. For BSCCO, they change linearly with the average vortex spacing, a_0 , which is proportional to the magnetic field ($a_0 \sim B^{-1/2}$) and decrease monotonically as the tilt angle increases. Secondly, the average number of vortices between chains, L_c/a_0 , for our samples decreases rapidly with φ and depends noticeably on B_{ext} , while in BSCCO it is nearly independent of both.

The main difference between YBCO and BSCCO, as far as the flux lattice behavior is concerned, lies in their substantially different anisotropy: $\gamma = 5 - 8$ for YBCO and > 150 for BSCCO. It reflects a difference in coupling between the superconducting Cu-O layers: it is generally accepted that in YBCO the coupling is strong enough for vortices to behave as 3D objects, and the FLL in this material is well described by the anisotropic London theory. In BSCCO a much weaker coupling leads to the formation of 2D vortices ("pancakes") and the 3D London theory is replaced by the Lawrence-Doniach model.⁸ In particular, detailed calculations of the FLL geometry in tilted fields showed that in cases of very high anisotropy, such as in BSCCO or Ta-Ba-Ca-Cu-O, the tilted lattice in the vicinity of H_{c1} should transform into a new vortex ar-

range, the so-called combined lattice, which consists of two sets of coexisting vortices: parallel and perpendicular to the \hat{c} axis.⁸ This division of the FLL into two species was proposed as an explanation of the peculiar chain structure observed in BSCCO which may be a result of the interaction between the two sets of vortices.⁶ It is, however, unlikely to explain the coexistence of vortex chains and the intervening FLL in the present experiment. First, because doping of YBCO with Al, Fe, or Co does not affect the anisotropy at all (according to the measurements of H_{c2} in Fe-doped samples¹⁰) or affects it only slightly (according to the measurements of λ_c and λ_{ab} from ac susceptibility of Co-doped YBCO:¹⁶ for the Co content $x = 0.04$, $\gamma = 10$ was found, while for the pure YBCO the same measurements have given $\gamma = 7.5$). Second, the minimum in the angular dependence of a_c (Fig. 3) contradicts this scenario because the latter would mean $\sim B_0^{-1/2}$ scaling of *all* vortex spacings with the applied field, as was the case in BSCCO.

Recently, an alternative proposal has been advanced.⁷ By taking into account the boundary conditions imposed by the slab geometry, typical of copper oxide single crystals, Daemen *et al.* have shown that the appropriate thermodynamic potential is a minimum when some of the vortices lie parallel to the \hat{c} axis while others lie at an oblique angle to it. In this case, the coexistence of the two vortex species should become favorable in *higher* fields starting from some minimum field H_{cr} . It is the magnitude of H_{cr} that defines the difference between the vortex chain states in BSCCO and YBCO: for YBCO it is estimated as ≈ 200 Oe, much larger than the largest field used in the experiment,⁴ while for BSCCO H_{cr} is as low as 30 Oe.

As far as the present study is concerned, this recent proposal produces a natural explanation for the angular dependence of both the intrachain vortex spacing, a_c , and the distance between chains, L_c (the latter, in other words, represents the fraction of chains in the mixture). However, we have not found any evidence of the existence of H_{cr} which is inherent in this model. The mixture of chains and the FLL was observed for the fields as low as $H_{\text{ext}} = 10$ Oe, which corresponds to $B_0 = 3 - 4$ G, depending on φ . At the same time, the magnitude of the critical field in our case should be similar to that for YBCO, i.e., much larger than the fields we used in the experiment.

We believe that the coexistence of the vortex chains and the FLL in our samples represents a metastable vortex state, i.e., it is a result of the competition between vortex attraction, which tends to form a pure chain state, and pinning, which reduces the vortex mobility. As the superconductor is cooled down, a high mobility is required for vortices to rearrange from the isotropic FLL, which nucleates at T_c , to an equilibrium state at lower temperatures—vortex chains. For instance, strong pinning by twins in YBCO completely eliminated any sign of the effects considered here.¹⁵ One can conclude from the fairly disordered FLL in Fig. 1 that collective (bulk) pinning is definitely more effective than in the twin-free YBCO. However, the more relevant characteristic, as far as formation of the vortex chains is concerned, must be

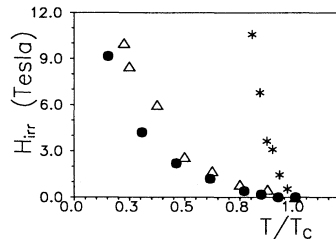


FIG. 4. Irreversibility field vs reduced temperature for our Al-YBCO crystals (●). For the sake of comparison, data from Ref. 17 for pure (twinned) YBCO (*) and 4% Co-doped YBCO (Δ) are also shown.

the irreversibility temperature rather than just the strength of bulk pinning. In pure YBCO, although pinning was low and the FLL exhibited long-range order, the pattern of vortex chains was “frozen in” close to T_c —at $T^*/T_c = 0.83$ – 0.88 .⁴ The irreversibility temperature for YBCO at the relevant field 50 G is higher still: $T_{irr}/T_c \approx 0.998$. Therefore, one can assume that the domain in the H - T phase diagram, where vortices are mobile enough to reach their positions of lowest energy, includes the region of reversible behavior plus a portion of the H - T plane immediately below the irreversibility line, where pinning is still low. [Note that the critical current in high- T_c superconductors decreases with temperature as $J_c \propto \exp(-T/T_0)$.] Remarkably, the irreversibility temperature is shifted greatly by Al doping. Figure 4 shows the irreversibility line calculated from our measurements of irreversible magnetization, where $H_{irr}(T)$ was defined by the onset of detectable irreversibility of dc magnetization [the experimental error is about 10% (Ref. 17)]. At 50 G, the irreversibility temperature estimated as the temperature where the field cooling and zero-field-cooling magnetization curves separate, was $T_{irr}(50 \text{ G})/T_c = 0.9$ – 0.92 , also lower than in YBCO. Thus, the wider region of reversible behavior gives the vortices more room for maneuver towards their equilibrium positions that can partly compensate for the more effective pinning in our samples.

A rapid and monotonic decrease of the number of vortex rows locked between chains, L_c/a_0 , with φ [Fig. 3(b)] would also seem to conform with this scenario. In other words, it corresponds to a rapid increase in the fraction of the sample volume occupied by the vortex chains and can be interpreted as an increase in the average distortion of the isotropic FLL imposed by tilt. On the other hand,

a monotonic increase of the distortion of the FLL unit cell on increasing the tilt is expected from the numerical calculations of the vortex geometry in tilted fields.³ Finally, a further argument is given by the following consideration. If, as argued above, the FLL vortices would have rearranged into chains provided there was no pinning, then an area occupied by each of the chain vortices must be equal to the area per one vortex of the intervening FLL:¹⁸ $S_{ch}/N_{ch} = (S - S_{ch})/(N - N_{ch})$, where S_{ch} is the area occupied by the vortex chains; N_{ch} is the number of chain vortices; S is the total area analyzed and N is the total number of vortices. Analysis of the decoration patterns for different tilt angles and fields have shown that the above relation always holds to a good accuracy. For example, for $H_{ext} = 20$ Oe, $\varphi = 63^\circ$ [Fig. 2(a)] we get $S_{ch}/N_{ch} = (1.92 \pm 0.11) \times 10^{-8} \text{ cm}^2$ and $(S - S_{ch})/(N - N_{ch}) = (2.0 \pm 0.11) \times 10^{-8} \text{ cm}^2$; for $\varphi = 75^\circ$, $H_{ext} = 40$ Oe, respective numbers are $(1.97 \pm 0.07) \times 10^{-8} \text{ cm}^2$ and $(2.04 \pm 0.07) \times 10^{-8} \text{ cm}^2$, etc. (the accuracy of the vortex spacing measurements is taken $0.2a_0$).

In summary, direct observations of the vortex structure of 4% Al-doped YBCO in tilted magnetic fields were performed using the decoration technique. For high tilt angles, between 50° and 80° the usual FLL transformed into the new vortex phase looking similar to the one observed in the highly anisotropic BSCCO: vortex chains running in the direction of tilt and embedded into the FLL oriented parallel to them. The intra- and interchain vortex spacings depended strongly on the tilt angle and only weakly on the applied field. These dependencies, very different from those for BSCCO, indicate that the chains originate from the anisotropy-induced vortex attraction and the observed vortex phase is a new one which can be described as intermediate between the pure chain state in twin-free YBCO and commensurate arrays of vortex chains in BSCCO. The coexistence of vortex chains with the FLL is attributed to the effect of pinning which reduces the vortex mobility during the sample cooling and does not allow complete transition from the isotropic FLL to the pure chain state.

We are indebted to Y. Liang for providing the possibility to perform magnetization measurements and to D. N. Zheng for his help with these measurements. We also wish to thank V. Kogan for many helpful discussions. This work was supported by the Science and Engineering Research Council of the United Kingdom.

*On leave from the Institute of Solid State Physics, Russian Academy of Sciences, 142432 Chernogolovka, Russia.

¹A. M. Grishin *et al.*, Zh. Eksp. Teor. Fiz. **97**, 1930 (1990) [Sov. Phys. JETP **70**, 1089 (1990)].

²A. I. Buzdin and A. Yu. Simonov, Zh. Eksp. Teor. Fiz. **98**, 2074 (1990) [Sov. Phys. JETP **71**, 1165 (1990)]; Physica C **175**, 143 (1991).

³L. L. Daemen *et al.*, Phys. Rev. B **46**, 3631 (1992).

⁴P. L. Gammel *et al.*, Phys. Rev. Lett. **68**, 3343 (1992).

⁵C. A. Bolle *et al.*, Phys. Rev. Lett. **66**, 112 (1991).

⁶D. A. Huse, Phys. Rev. B **46**, 8621 (1992).

⁷L. L. Daemen *et al.*, Phys. Rev. Lett. **70**, 2948 (1993).

⁸L. N. Bulaevskii *et al.*, Phys. Rev. B **46**, 366 (1992).

⁹See, for example, S. Semenovskaya *et al.*, Phys. Rev. B **47**,

12 182 (1993), and references therein.

¹⁰M. D. Lan *et al.*, Phys. Rev. B **47**, 457 (1993).

¹¹R. Wordenweber *et al.*, J. Appl. Phys. **65**, 1648 (1989); R. Wordenweber *et al.*, Supercond. Sci. Technol. **2**, 207 (1989).

¹²K. Sasaki *et al.* (unpublished).

¹³C. P. Bean, Rev. Mod. Phys. **36**, 31 (1964); E. M. Gyorgy *et al.*, Appl. Phys. Lett. **55**, 283 (1989).

¹⁴I. V. Grigorieva *et al.*, Physica C **199**, 73 (1992).

¹⁵I. V. Grigorieva, L. A. Gurevich, and L. Ya. Vinnikov, Physica C **195**, 327 (1992).

¹⁶A. Porch, J. R. Cooper, D. N. Zheng, J. R. Waldram, A. M. Campbell, and P. A. Freeman, Physica C **214**, 350 (1993).

¹⁷D. N. Zheng *et al.*, Supercond. Sci. Technol. **5**, S495 (1992).

¹⁸V. Kogan (private communication).

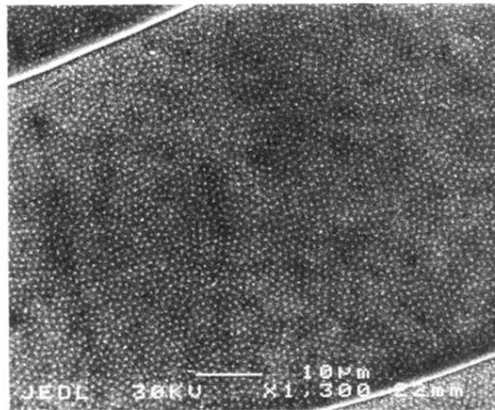


FIG. 1. Scanning electron microscopy (SEM) micrograph of the FLL in the magnetic field of 20 G applied parallel to the \hat{c} axis.

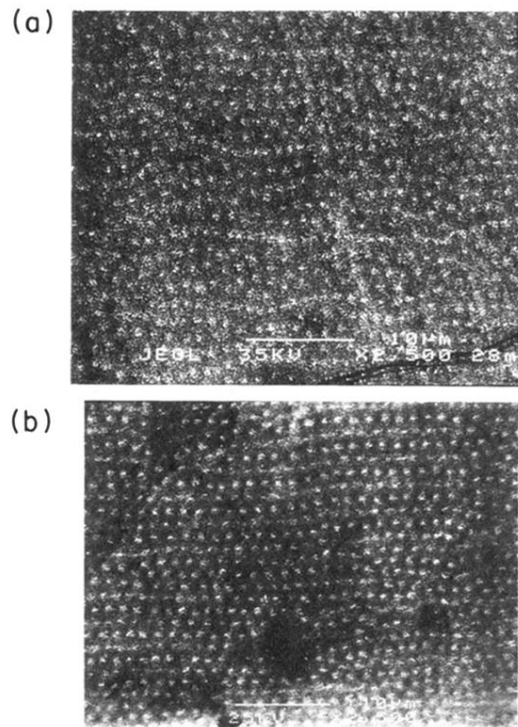


FIG. 2. SEM images of the vortex chains-FLL mixture for the same normal component of the applied field, $B_0 \approx 10$ G, and two tilt angles: (a) $\varphi = 63^\circ$, (b) $\varphi = 80^\circ$. The (\mathbf{B}, \hat{c}) plane in the micrographs is horizontal.